Structural insights into mRNA reading frame regulation by tRNA modification and slippery codon-anticodon pairing

Eric D. Hoffer[1], Samuel Hong[1], S. Sunita[1], Tatsuya Maehigashi[1], Ruben L. Gonzalez, Jr.[2]

Paul Whitford[3] and Christine M. Dunham[1]

[1]Department of Biochemistry, Emory University School of Medicine, Atlanta, GA, USA

[2]Department of Chemistry, Columbia University, New York, NY, USA

[3]Department of Physics, Northeastern University, Boston, MA, USA

Contact: Christine M. Dunham, christine.m.dunham@emory.edu, phone +1-404-712-1756, fax +1-404-727-2738.

Data deposition: Crystallography, atomic coordinates, and structure factors have been deposited in the Protein Data Bank, www.pdb.org (PDB codes 6NTA, 6NSH, 6NUO, 6NWY, 6O3M, 6OSI)

Key words: ribosome, frameshift, near cognate, mRNA, tRNA, fidelity, translation

ABSTRACT

Modifications in the tRNA anticodon, adjacent to the three-nucleotide anticodon, influence translation fidelity by stabilizing the tRNA to allow for accurate reading of the mRNA genetic code. One example is the N1-methylguaonosine modification at guanine nucleotide 37 (m^1G37) located in the anticodon loop, immediately adjacent to the anticodon nucleotides 34-36. The absence of m^1G37 in $tRNA^{Pro}$ causes +1 frameshifting on polynucleotide, slippery codons. Here, we report structures of the bacterial ribosome containing $tRNA^{Pro}$ bound to either cognate or slippery codons to determine how the m^1G37 modification prevents mRNA frameshifting. The structures reveal that certain codon-anticodon contexts and m^1G37 destabilize interactions of $tRNA^{Pro}$ with the peptidyl site, causing large conformational changes typically only seen during EF-G mediated translocation of the mRNA-tRNA pairs. These studies provide molecular insights into how m^1G37 stabilizes the interactions of $tRNA^{Pro}$ with the ribosome and the influence of slippery codons on the mRNA reading frame.

26 **IMPACT STATEMENT**

27 Chemical modifications near the tRNA anticodon and specific mRNA-tRNA pairs combine to control the
28 ribosomal three-nucleotide mRNA reading frame, essential for the sequential addition of amino acids into
29 polypeptide chains.

30 **INTRODUCTION**

31 Post-transcriptionally modified RNAs, including ribosomal RNA (rRNA), transfer tRNA (tRNA) and
32 messenger RNA (mRNA), stabilize RNA tertiary structures during ribonucleoprotein biogenesis, regulate
33 mRNA metabolism, and influence other facets of gene expression. RNA modifications located in the three-
34 nucleotide anticodon of tRNAs contribute to accurate protein synthesis and expand tRNA coding capacity
35 by facilitating Watson-Crick-like base-pairs with mRNA codons. The most commonly modified tRNA
36 position is at nucleotide 34 and the modifications to this nucleotide are functionally important for gene
37 expression by facilitating base-pairing interactions with the mRNA codon to expand the tRNA coding
38 capacity (*1-3*). Other tRNA nucleotides also contain highly conserved nucleotide modifications, but their
39 precise roles in protein synthesis are not fully understood. For example, nucleotide 37 is adjacent to the
40 anticodon (Figure 1A) and is modified in >70% of all tRNAs (*4*). The two most common modifications at
41 nucleotide 37 are 6-threonylcarbamoyladenosine (t^6A) and 1-methylguanosine (m^1G), which together
42 account for more than 60% of nucleotide 37 modifications (*2*). Both the t^6A37 modification in $tRNA^{Lys}$ and
43 the m^1G37 modification in $tRNA^{Pro}$ are thought to stabilize the tertiary structure of the anticodon loop for
44 high-affinity binding to their cognate codons (*5-7*). The m^1G37 modification also prevents the ribosome
45 from shifting out of the three-nucleotide mRNA codon frame ('frameshifting') to ensure the correct
46 polypeptide is expressed (*8-11*). However, the molecular basis for how the m^1G37 modification maintains
47 the mRNA reading frame is unknown.

48 The m^1G37 modification is present in >95% of all three $tRNA^{Pro}$ isoacceptors across all three
49 domains of life (*2, 8*). The absence of m^1G37 in $tRNA^{Pro}$ causes high levels of +1 frameshifting on so-called
50 'slippery' or polynucleotide mRNA sequences where four nucleotides encode for a single proline codon
51 (*8*). In the case of the $tRNA^{Pro}_{CGG}$ isoacceptor, a +1 slippery codon consists of the CCC proline codon and
52 either an additional C or U to form a four-nucleotide codon, CCC-(U/C) (*12, 13*) (codons depicted 5'- to
53 3'). $tRNA^{Pro}_{CGG}$ lacking m^1G37 results in the ribosome being unable to distinguish a correct from an incorrect
54 codon-anticodon interaction during decoding at the aminoacyl (A) site (*7, 14*). However, this miscoding
55 event does not cause the shift in the mRNA frame in the A site despite the $tRNA^{Pro}_{CGG}$ anticodon stem-loop

56 nucleotides become more mobile (*14*). A post-decoding frameshift event is further supported by detailed
57 kinetic analyses (*11*). The absence of the m^1G37 modification in $tRNA^{Pro}$ causes both a ~5% frameshifting
58 frequency during translocation of the mRNA-tRNA pair from the A to the peptidyl (P) site and ~40%
59 frameshifting frequency once the mRNA-tRNA pair has reached the P site. When $tRNA^{Pro}_{CGG}$ lacks m^1G37
60 and decodes a +1 slippery codon, both the process of translocation and the unique environment of the P site
61 appear to contribute to the inability of the ribosome to maintain the mRNA frame.

62 In circumstances where mRNA frameshifting is caused by changes in the tRNA such as the absence
63 of modifications or changes in the size of the anticodon loop as found in frameshift suppressor tRNAs,
64 primer extension assays demonstrated that the shift into the +1 frame is observed upon direct tRNA binding
65 at the P site (*15, 16*). These studies clearly demonstrate that the nature of the interactions between the
66 frameshift-prone mRNA-tRNA pair and the ribosomal P site directly permit frameshifting. Furthermore,
67 the presence of a nascent polypeptide chain, the acylation status of the tRNA (deacylated or aminoacylated),
68 and even the presence of a tRNA in the A site do not contribute to the ability of the tRNA to cause
69 frameshifting. Structural studies of frameshift-prone or suppressor tRNAs have provided molecular insights
70 into how such tRNAs may dysregulate mRNA frame maintenance (*14, 17, 18*). Frameshift suppressor
71 $tRNA^{SufA6}$ contains an extra nucleotide in its anticodon loop and undergoes high levels of +1 frameshifting
72 on slippery proline codons (*8, 13*). The structure of the anticodon stem-loop (ASL) of the $tRNA^{SufA6}$ bound
73 directly at the P site revealed that its anticodon engages the slippery CCC-U proline codon in the +1 frame
74 (*18*). Further, the full-length $tRNA^{SufA6}$ bound at the P site reveals that the small 30S subunit head domain
75 swivels and tilts, a similar movement to that caused by GTPase elongation factor-G (EF-G) upon
76 translocation of the tRNAs through the ribosome (*19-22*). The process of mRNA-tRNA translocation is
77 coupled to this head domain swivel and tilt which is distinct from other conformational changes the
78 ribosome undergoes including intersubunit rotation (*21, 23-27*). However, the 70S-$tRNA^{SufA6}$ structure is
79 in the absence of EF-G, suggesting that a +1 frameshift event caused by frameshift-prone tRNAs
80 dysregulates some aspect of translocation. Although these studies demonstrate that +1 frameshift-prone
81 tRNAs are good model systems to uncover mechanisms by which both the ribosome and the mRNA-tRNA

82 pair contribute to mRNA frame maintenance, it is unclear whether normal tRNAs lacking modifications
83 result in +1 frameshifting in the same manner. To address this question, here we solved six 70S structures
84 of $tRNA^{Pro}_{CGG}$ in the presence or absence of the m^1G37 modification and bound to either cognate or slippery
85 codons in the P site. Our results define how the m^1G37 modification stabilizes the interactions of $tRNA^{Pro}_{CGG}$
86 with the ribosome. We further show that ribosomes bound to mRNA-tRNA pairs that result in +1
87 frameshifts promoted by $tRNA^{Pro}_{CGG}$ result in large conformational changes of the 30S head domain,
88 consequently biasing the tRNA-mRNA pair towards the E site.
89
90 **RESULTS**
91 **A near-cognate interaction between ASL^{Pro} and the slippery CCC-U proline codon *alone* causes a**
92 **shift into the +1 frame.** To address whether $tRNA^{Pro}_{CGG}$ induces a +1 frameshift by a similar mechanism as
93 $tRNA^{SufA6}$, we determined two X-ray structures of ASL^{Pro} decoding either a cognate CCG or a near-cognate,
94 slippery CCC-U codon bound at the P site (Figure 1 and Tables 1 and 2). We used chemically synthesized
95 ASL^{Pro} (17 nucleotides) to ensure G37 is fully methylated at the N1 position (Figure 1A). The structure of
96 P-site ASL^{Pro} interacting with a cognate CCG proline codon was solved to a resolution of 3.1 Å and reveals
97 that the three nucleotides of the anticodon (nucleotides G36-G35-C34) form three Watson-Crick base-pairs
98 with the C_{+1}-C_{+2}-G_{+3} mRNA codon, respectively (Figure 1A) (mRNA nucleotides are numbered starting at
99 +1 from the P-site codon). The anticodon interacts with the codon in the canonical or 0 mRNA frame
100 indicating a frameshift has not occurred.
101 We next asked how ASL^{Pro} interacts in the P site with a near-cognate CCC-U codon, a slippery
102 codon known to facilitate +1 frameshifts (*8, 11*). In this X-ray structure solved to a resolution of 3.4 Å, we
103 find two different conformations of the codon-anticodon interaction in the two molecules of the
104 crystallographic asymmetric unit (Figures 1C and D and Table 2 and Video 1). Although it is common for
105 one 70S ribosome to contain better electron density than the other in the asymmetric unit in this particular
106 crystal form (*28*), to our knowledge, it is not common to obtain two different conformational states of the
107 same functional complex. In the first ribosome molecule, nucleotides G36 and G35 of ASL^{Pro} form Watson-

108 Crick base-pairs with the first two nucleotides of the 0-frame mRNA codon (Figure 1C). A mismatch
109 C_{+3}•C34 forms at the third base-pair position of the codon-anticodon interaction and contains a single
110 hydrogen bond between the Watson-Crick face of C_{+3} (the N3 position) and C34 (the N4 position). This
111 codon-anticodon interaction is thus defined as near cognate because of the single mismatch. The distance
112 between the anticodon nucleotide C34 and the mRNA nucleotide C_{+3} is increased in the P site as compared
113 to this same mRNA-tRNA pair in the A site (3.6 Å versus 3.1 Å (*14*)), indicating that the interaction has
114 weakened. Although this interaction is at the distance limit of a hydrogen bond, C34 and C_{+3} are positioned
115 to form a *cis*-Watson-Crick pair, similar to the orientation observed in the A site (*14*) (Figure 1C-figure
116 supplement 1). The codon-anticodon interaction is in the 0 frame as indicated by the clear phosphate density
117 of the next mRNA nucleotide, U_{+4} (Figure 1C-figure supplement 1). The mRNA used in these studies only
118 contained a single nucleotide after the three-nucleotide codon programmed in the P site to allow for the
119 unambiguous identification of the reading frame.

120 Strikingly, in the other ribosome molecule in the crystallographic asymmetric unit, the codon-
121 anticodon interaction is in the +1 frame (Figure 1D and Video 1). The first two nucleotides of the anticodon
122 (G36-G35) form Watson-Crick base-pairs with C_{+2}-C_{+3} nucleotides of the mRNA codon, respectively. The
123 first nucleotide of the proline codon, C+1, no longer interacts with the tRNA and does not appear to make
124 any interactions with the ribosome. At the third position of the codon-anticodon interaction, a *cis*-Watson-
125 Crick U_{+4}•C34 pair forms that contains a single hydrogen bond between the Watson-Crick face of U_{+4} (the
126 O4 position) and C34 (the N4 position) (Figure 1D-figure supplement 1C). The absence of electron density
127 for a subsequent nucleotide in the mRNA confirms the +1 frame of the codon-anticodon interaction as this
128 is the last nucleotide of the mRNA (Figure 1D-figure supplement 1C). Therefore, although the m^1G37
129 modification is present in ASL^{Pro}, the shift in the +1 frame can still occur. These data indicate that the
130 presence of a near-cognate, slippery codon is sufficient to promote a +1 shift in the mRNA frame.
131 Consistent with our observations, biochemical studies of other near-cognate mRNA-tRNA pairs in the P
132 site that also show frameshifting in both directions on the mRNA (*29*).
133

134 **The absence of m^1G37 in $tRNA^{Pro}_{CGG}$ bound to a cognate CCG codon does not destabilize its interactions**
135 **with the ribosome.** We next asked how full-length $tRNA^{Pro}_{CGG}$ bound at the P site interacts with the mRNA.
136 Our recent structure of the ribosome with +1 frameshift suppressor $tRNA^{SufA6}$ indicated that although the
137 tRNA was positioned at the P site, when engaged with mRNA that causes +1 frameshifts, the tRNA moves
138 towards the E site and induces large conformational changes of the 30S subunit, specifically the head
139 domain (*18*). We wanted to directly compare these structures given that the +1 frameshift is induced by
140 different signals: an extra nucleotide in the anticodon loop in $tRNA^{SufA6}$ and the absence of m^1G37 in tRNA
141 $^{Pro}_{CGG}$. It is possible that $tRNA^{SufA6}$ causes this destabilization and thus conformational changes of the 30S head
142 domain because of the extra nucleotide in its ASL; such a mechanism would likely not apply for m^1G37 in
143 $tRNA^{Pro}_{CGG}$. As a control, we solved a structure of $tRNA^{Pro}_{CGG}$ containing the m^1G37 modification bound to a
144 cognate CCG codon in the ribosomal P site to a resolution of 3.2 Å (Figure 2A and Table 3 and Video 2).
145 $tRNA^{Pro}_{CGG}$ binds in the classical P/P state (bound to the P site on the 50S and the 30S) and interacts with the
146 proline codon in the 0 frame. Specifically, the G36-G35-C34 anticodon nucleotides form three Watson-
147 Crick base-pairs with the C_{+1}-C_{+2}-G_{+3} proline codon nucleotides, respectively (Figure 2E-figure supplement
148 1A and 1B). The methyl group at position 1 of the nucleobase of G37 stacks with the nucleobase of
149 anticodon nucleotide G36 to form a canonical four-nucleotide stack between nucleotides 34-37. This
150 anticodon stack is important for productive interactions with both mRNA and the ribosome (*14, 30, 31*).
151 The P/P location of $tRNA^{Pro}_{CGG}$ is thus consistent with functional assays demonstrating that $tRNA^{Pro}$
152 isoacceptors do not appear to spontaneously move into the +1 frame on non-slippery codons (*8, 11*).
153 We next solved a 3.9 Å structure of $tRNA^{Pro}_{CGG}$ lacking the m^1G37 modification (G37 Δm^1) and
154 interacting with a cognate CCG proline codon in the P site (Figure 2B-figure supplements 1C and 1D and
155 Table 3 and Video 2). Although the m^1G37 modification was previously shown to be critical for high-
156 affinity binding and decoding of the cognate CCG codon at the A site (*7*), its influence on the overall
157 conformation of $tRNA^{Pro}_{CGG}$ in the P site appears to be minimal as the tRNA adopts a P/P orientation (Figure
158 2B). Notably, the mRNA remains in the 0 frame with three Watson-Crick base-pair interactions between
159 the codon and the anticodon (Figure 2F). Similar to the structural studies of the ASL^{Pro} in the 0 frame

160 (Figures 1B and D), the mRNA used in these studies contains an additional nucleotide after the P-site CCG
161 codon (Figures 1; Figure 2B and Table 1). The mRNA has clear phosphate density for the single A-site
162 nucleotide indicating the mRNA remains in the 0 frame (Figure 2-figure supplement 1D). The absence of
163 the m^1G37 modification correlates with a slightly weaker U32-A38 pairing when compared to modified
164 $tRNA^{Pro}_{CGG}$ (Figure 2-figure supplement 2B). These structures suggest that the absence of 1-methyl
165 modification on G37 alone is not sufficient to destabilize the tRNA in the P site of the ribosome. This
166 observation is also consistent with toeprint analyses demonstrating that $tRNA^{Pro}_{GGG}$ lacking m^1G37 on a non-
167 slippery codon remained in the 0 frame (*11*).
168
169 **A near-cognate, slippery proline codon in the P site causes $tRNA^{Pro}_{CGG}$ destabilization and 30S head**
170 **movement.** In an attempt to reconcile the exact role of the m^1G37 modification in $tRNA^{Pro}_{CGG}$ in the context
171 of a near-cognate, slippery codon, we next solved a ribosome structure in the presence of m^1G37 modified
172 $tRNA^{Pro}_{CGG}$ in the P site bound to a near-cognate, slippery CCC-U codon to a resolution of 3.2 Å (Figure 2C
173 and Table 3 and Video 2). Unexpectedly, $tRNA^{Pro}_{CGG}$ moves from the P site towards the E site, adopting a
174 position on the ribosome which we refer to as e*/E (*18*) (where lowercase e* signifies an intermediate
175 position between the 30S subunit P and the E sites and a 50S E-site position) (Figure 2C-figure supplement
176 1E). The e*/E position of $tRNA^{Pro}_{CGG}$ when bound to this near-cognate, slippery codon is different from the
177 classical P/P position that the same tRNA adopts when it interacts with a cognate CCG codon (compare
178 Figure 2A with 2C). The classical P/P $tRNA^{Pro}_{CGG}$ location on its cognate codon is consistent with dozens of
179 other P-site tRNA-ribosome structures. Therefore, the ability of $tRNA^{Pro}_{CGG}$ to move towards the E site when
180 bound to a slippery proline codon suggests that it is this near-cognate codon-anticodon interaction alone
181 that is sufficient to destabilize $tRNA^{Pro}_{CGG}$ (Figure 2C).
182 The e*/E position of the $tRNA^{Pro}_{CGG}$-mRNA pair is additionally coupled to large conformational
183 changes of the 30S head domain (Figure 3 and Video 2). 30S head motions accompanying canonical
184 translocation or caused by a frameshift-prone tRNAs have been previously described by our group and
185 others in terms of the degree of swivel and tilt (*18, 23-25, 32, 33*), but these two distinct movements have

never been analyzed separately (Figure 3). To more precisely describe this multidimensional motion, we used previously reported procedures to define "swivel" as the movement of the head relative to the body within a plane (*i.e.* pure rotation about a single axis defined by structures of the unrotated and swiveled conformations (PDB codes 4V9D and 4V4Q, respectively)), while "tilt" describes any deviations from pure rotation (*34*). Together, these more accurate calculations provide an unambiguous description of the full, three-dimensional orientation of the head during translocation, where the tRNAs are found in intermediate states (*24, 25*). The head domain swivels in a ~18° counterclockwise direction while also undergoing a ~5° tilt away from the ribosome and perpendicular to the mRNA path (*23-25*) (the counterclockwise swivel is defined with the ribosome viewed with E, P, A tRNA sites oriented from left to right as depicted in Figure 2). The head domain is comprised of 16S rRNA nucleotides 930-1380 and seven ribosomal proteins (S3, S7, S9, S10, S13, S14, and S19) that collectively move as a rigid body during EF-G-mediated translocation of the mRNA-tRNA pairs on the 30S (*23-25*). The same swivel and tilting of the head domain of e*/E tRNA $^{Pro}_{CGG}$ occurs but in our structure lacks EF-G. This structure indicates that even with the m^1G37 modification, interactions of $tRNA^{Pro}_{CGG}$ with the P site are destabilized when bound to a near-cognate codon, promoting its movement towards the E site along with 30S head domain swiveling and tilting.

The mRNA located in the 30S E and P sites is constricted when $tRNA^{Pro}_{CGG}$ adopts an e*/E position. The path of the mRNA on the ribosome accommodates three nucleotides, or a single codon, in each of the A, P and E sites (Figures 4A and B). The ribosome interacts extensively with the mRNA in the A site to ensure accurate decoding but interacts less substantially with the P-site codon, while the E-site mRNA codon is the least monitored. The ribosome interacts with mRNA in the E site at two positions through non-sequence specific interactions: 16S rRNA nucleotide G693 stacks with the first nucleotide of the E-site mRNA codon and the G926 nucleobase contacts the phosphate of the third mRNA codon nucleotide (Figures 4B and C) (*28*). The e* position of $tRNA^{Pro}_{CGG}$ signifies that the tRNA is closer to the E site than the P site on the 30S, however it is similar to the pe/E tRNA position seen in translocation intermediate ribosome structures containing EF-G (Figure 4D) (*25*). Only two nucleotides of the codon-anticodon interaction of the pe/E

212 tRNA are positioned in the E site leaving a pocket for an additional nucleotide to occupy upon full
213 translocation of the mRNA-tRNA pair (*24, 25*) (compare Figures 4C with 4D). In our structure containing
214 an e*/E $tRNA^{Pro}_{CGG}$ bound to a near-cognate, slippery codon, the first three nucleotides of the codon fully
215 occupy the E site (Figure 4E), despite the codon-anticodon adopting an intermediate position on the 30S
216 between the P and the E sites. This compaction of the mRNA means there is no space for the entire four
217 nucleotide codon in the E site upon translocation of the mRNA-tRNA pair. Additionally, the mRNA path
218 5' from the E site turns sharply by ~100° as the mRNA transits to the outside of the ribosome (Figure 4C).
219 In the case of e*/E $tRNA^{Pro}_{CGG}$, upon full translocation of the mRNA-tRNA pair to the E site, the first
220 nucleotide of the codon would be displaced from the E site to accommodate the three-nucleotide codon or
221 the last three nucleotides of the CCC-U codon. This placement would position the mRNA in the +1 frame.
222 The mRNA boundary between the P and the E sites on the 30S subunit appears to be demarcated
223 by 16S rRNA nucleotide G926 (Figures 4B and 4C) (*28*). G926 interacts with the phosphate of the +3
224 nucleotide of the E-site codon thus defining its 3'-end (Figure 4C). In our structure of $tRNA^{Pro}_{CGG}$ interacting
225 with a near-cognate, slippery codon, G926 instead interacts with U_{+4} of the CCC-U codon rather than the
226 third nucleotide, thereby defining U_{+4} as the end of the E-site codon (Figure 4E). Even in translocation
227 intermediate ribosome structures containing EF-G, G926 interacts with the +3 phosphate of the mRNA,
228 although this ribosome complex contains a cognate mRNA-tRNA pair (Figure 4D) (*25*). Comparison of
229 post-translocation (*35*), translocation intermediate (*24, 25*), and our structure presented here reveals that the
230 position of G926 in all three is very similar, while the position of the mRNA changes substantially (Figures
231 4C, D and E). In summary, although $tRNA^{Pro}_{CGG}$ is fully translocated to the E site in our new structure, the
232 four-nucleotide mRNA codon is compacted in the E site as if translocation has already taken place (Figure
233 4E).
234
235 **The G966-C1400 bridge connecting the 30S head and body domains is broken in the presence of a**
236 **near-cognate codon-anticodon interaction.** The ribosome minimally interacts with the mRNA-tRNA pair
237 in the P site: 16S rRNA C1400 contacts G966 and stacks with the third base-pair of the codon-anticodon

238 (Figure 5A) (*28*). The G966-C1400 pair remains intact during translocation of the mRNA-tRNA pair from
239 the P to the E site as part of the head domain, as evidenced by ribosome structures in translocation
240 intermediate states containing EF-G (Figure 5B). (*24, 25*). In our structure containing e*/E $tRNA^{Pro}_{CGG}$ bound
241 to a near-cognate, slippery codon, the G966-C1400 interaction is ablated (Figure 5C). Since the G966-
242 C1400 interaction is effectively the bridge between the head and body domains, this disruption can be
243 attributed to a dysregulation caused by this spontaneous translocation event.
244
245 **The absence of the m^1G37 modification in $tRNA^{Pro}_{CGG}$ coupled with a near-cognate, slippery codon-**
246 **anticodon interaction causes complete disordering of the 30S head domain.** Finally, we solved a 4.1 Å
247 structure of $tRNA^{Pro}_{CGG}$ lacking m^1G37 (Δm^1) interacting with a near-cognate, slippery CCC-U codon at the P
248 site. The electron density for majority of the $tRNA^{Pro}_{CGG}$ on the 50S subunit is well-resolved, indicating that,
249 like the analogous structure solved in the presence of the m^1G37 modification (Figure 2C), the tRNA has
250 also moved towards the E site on the 50S subunit (Figure 2D). In contrast, the electron density is weak the
251 $tRNA^{Pro}_{CGG}$ ASL and E-site mRNA indicating these regions are dynamic in the context of slippery codon and
252 in the absence of m^1G37 modification (Figure 2D-figure supplement 2G). Disordering of $tRNA^{Pro}$ G37
253 (Δm^1) starts approximately at the beginning of the anticodon loop at nucleotides U32-A38.
254 Correspondingly, the 30S head domain region is also disordered (Figure 2D-figure supplement 3D),
255 whereas the only region of the 30S body domain with poor electron density is the P/E loop nucleotides
256 G1338 and A1339. Taken together, in this mRNA-tRNA pairing that causes high levels of frameshifting,
257 interactions with the tRNA are destabilized in the P site resulting in the codon-anticodon adopting an e*
258 location and high mobility of the 30S head domain.
259
260 **DISCUSSION**
261 The importance of tRNA modifications in protein synthesis has been recognized for decades, yet their
262 precise roles outside the anticodon have been elusive. Modifications in the anticodon loop at position 37 of

263 tRNAs have been implicated in mRNA frame maintenance (*10, 36*), but how absence of a single
264 modification can dysregulate the mRNA frame remained unclear. Here, we elucidated the role of the m^1G37
265 modification in $tRNA^{Pro}_{CGG}$, which was known to be important in stabilizing stacking interactions with
266 anticodon nucleotides (*14*) and in the prevention of frameshifting (*8, 37*). We find that this single methyl
267 group influences the overall stability of $tRNA^{Pro}_{CGG}$ in an unexpected manner that causes large conformational
268 changes between the tRNA and the 30S head domain, a domain known to move extensively during
269 translocation of the tRNAs (*21, 23-25*). However, the methylation *alone* does not stabilize $tRNA^{Pro}_{CGG}$ on the
270 ribosome and, instead, its position is heavily influenced by interactions with a distinct slippery proline
271 codon. Our structures of different mRNA-$tRNA^{Pro}_{CGG}$ pairs on the ribosome allows the first detailed
272 mechanistic insight into how mRNA frame maintenance is regulated by both the m^1G37 modification and
273 the stability of mRNA-tRNA interaction.

274 The location on the ribosome where frameshifting can occur is likely dependent on the type of
275 frameshift (in the positive or negative mRNA direction) and whether tRNA or mRNA causes the frameshift
276 (*38-41*). The ribosome itself can prevent the frameshift through inherent differences in how the ribosome
277 interacts with the tRNA-mRNA complex at the different tRNA binding sites and such differences could
278 potentially influence frameshifting by relaxing interactions, for example, between the codon and anticodon.
279 While the codon-anticodon interaction located in the 30S A site is strictly monitored by conserved 16S
280 rRNA nucleotides to select for cognate tRNA (*42*), there are comparatively few interactions with the codon-
281 anticodon when positioned within the P and E sites, underscoring their different functional roles during the
282 translation cycle. This relative absence of interactions in the P and E sites provides an opportunity for the
283 mRNA to shift out of frame. $tRNA^{Pro}$ isoacceptors frameshift either during translocation from the A to the
284 P site or after translocation in the P site (*11, 43*). Therefore we sought to capture the interactions of $tRNA^{Pro}$
285 during a frameshift event. The structure of ASL^{Pro} bound to a slippery codon in the P site reveals the codon-
286 anticodon interaction has shifted into the +1 frame indicating that the anticodon stem-loop interaction with
287 the mRNA codon alone is important (Figure 1D). This frameshift is likely possible because interactions
288 with the P-site tRNA are limited to only 16S rRNA nucleotides G1338 and A1339 (called the P/E loop

289 nucleotides) with the anticodon stem and 16S rRNA C1400 with the anticodon nucleotide 34 (Figure 5A-
290 figure supplement 1). The P/E loop appears to indirectly enforce the mRNA frame by gripping the P-site
291 tRNA and these interactions are maintained as the tRNA moves from the P site to a hybrid P/E state (*44*)
292 and then to a translocation intermediate pe/E state (*24*). In the structures of ASL^{Pro} interacting with the
293 mRNA in the 0 frame, there is well-resolved density for G1338 and A1339 (Figures 1B and C-figure
294 supplement 1A,1D,1G), while there is some disordering of these nucleotides in the context of ASL^{Pro} bound
295 to the near-cognate, slippery codon in the +1 frame (Figure 1-figure supplements 1C,1F,1I). The inability
296 for G1338 and A1339 to grip the anticodon stem when the codon-anticodon is in the +1 frame likely results
297 in the destabilization of full-length $tRNA^{Pro}$ in these frameshift competent contexts (Figures 2C and D).
298 Simulations of the ribosome undergoing large movements of the head domain during translocation
299 implicate nucleotides G1338 and A1339 in the coupling of 30S head dynamics and displacement of the P-
300 site tRNA towards the E site (*34*). Therefore, the lack of gripping by these nucleotides when a frameshift
301 event is located in the P site appears to bias $tRNA^{Pro}$ towards the E site which, in turn, causes the 30S head
302 domain to swivel and tilt as if EF-G were bound.

303 In addition to P/E loop nucleotides G1338 and A1339, 16S rRNA nucleotide G966 is also part of
304 the 30S head domain and stacks with wobble nucleotide 34 of the P-site tRNA anticodon (Figure 5A). The
305 30S head is connected to the body domain via the interactions of G966 with nucleotide C1400; the G966-
306 C1400 pair remains stacked beneath the P-site tRNA and follows the tRNA as it moves to a hybrid P/E
307 state and to a translocation pe/E intermediate state upon EF-G binding (Figure 5B) (*24, 25, 44*). In the case
308 of P-site ASL^{Pro} interacting with a near-cognate, slippery codon in the 0 or +1 frame, *cis*-Watson-Crick
309 interactions form between C_{+3}•C34 and U_{+4}•C34, respectively (Figure 1-figure supplements 1K,1L). Both
310 interactions appear to result in reduced stacking with C1400. In structures of full-length $tRNA^{Pro}$-mRNA
311 pairs that cause +1 frameshifting and destabilization at the P site, the G966-C1400 interaction is broken
312 (Figure 5C). Together, these results suggest a connection between the reduced interactions of G1338-A1339
313 and G966-C1400 with the tRNA that appear to influence the movement of the P-site tRNA towards the E
314 site.

315 Although neither C1400 nor G966 have previously been implicated in mRNA frame maintenance,
316 there is a functional link between the P/E loop nucleotides G1338 and A1339, and C1400-G966. 16S rRNA
317 nucleotides in the P site are generally more tolerable of mutations than the A-site 16S rRNA, although
318 substitution of G966 substantially reduces ribosome activity to ~10% despite the mutation not being lethal
319 (*45*). This G966 mutant is suppressed by a G1338A mutation, indicating that the G1338A mutation can
320 stabilize interactions with the P-site tRNA even in the absence of the C1400-G966 interaction.

321 The interactions observed between the codon and anticodon of ASL^{Pro} bound to either cognate or
322 near-cognate codons reveal the process of shifting into the +1 frame (Figure 1D). In the context of full-
323 length mRNA-tRNA pairs that cause +1 frameshifting, both pairs move from the P site to occupy a position
324 between the E and the P site (Figures 2C and D). This mRNA-tRNA placement is similar to the translocation
325 intermediate containing EF-G (*24*). In the structure presented containing an e*/E $tRNA^{Pro}$ with the EF-G
326 containing structures containing an pe/tRNA, the tRNA moves slightly away from the mRNA. In the e*/E
327 $tRNA^{Pro}_{CGG}$ structure, the first position of the codon-anticodon forms a Watson-Crick interaction but the
328 second and third nucleotides of the codon-anticodon are not within hydrogen bonding distances (Figure
329 2G). Interestingly, in the EF-G bound translocation intermediate structure, the codon-anticodon also is not
330 within bonding distance (*24*). These results suggest that it is the disruptive nature of moving between tRNA
331 binding sites that perturbs the interactions between the codon and anticodon and these interactions likely
332 reform once the transition to the next tRNA binding site is completed.

333 30S head domain conformational changes were first captured in ribosome structures of tRNAs
334 moving between the A to the P sites (ap/ap state) and between the P and the E sites (pe/E state) on the 30S
335 in the presence of EF-G (*24, 25, 44*). Upon EF-G binding, the head domain is predicted to first tilt and then
336 swivel in a counterclockwise manner (as viewed when looking at the ribosome with E, P, A tRNA sites
337 from left to right as depicted in Figure 2) to translocate the two tRNAs to final E/E and P/P positions (*21,*
338 *34*). The departure of EF-G and reverse tilting of the head back towards the intersubunit space is followed
339 by clockwise swivel, the rate-limiting step for translocation (*21*). Frameshift-prone tRNAs, such as tRNA
340 $^{Pro}_{CGG}$, cause spontaneous head swiveling and tilting once the tRNA occupies the P site after the mRNA

341 frameshift has occurred. The inability of the ribosome to hold the P-site tRNA is influenced by weakening
342 of the interactions of the P/E loop with the anticodon stem and by disruption of the C1400-G966 interaction,
343 both events likely major contributors to the dysregulation of the 30S head domain. In other words, the head
344 domain is unable to maintain extensive interactions with the P-site tRNA and this failure leads to
345 spontaneous translocation. Single molecule FRET (smFRET) studies of translocation also show that upon
346 tRNA movement from the P to the E site, there is increased dissociation of the tRNA from the ribosome,
347 bypassing the post-translocation E/E state (*21*). These data seem to indicate that even during canonical
348 translocation from the P to the E site, this is a highly dynamic process which leads to destabilized tRNA.
349 Consistent with these observations, we would expect that once EF-G fully translocates $tRNA^{Pro}_{CGG}$ to the post
350 E/E state, there may be further decrease in interaction between the tRNA and ribosome. Additionally, our
351 structures show 30S head swiveling and tilting, in the absence of EF-G, concurrent with the +1 frameshift
352 event would likely prevent EF-G from binding. EF-G residues located in the tip of domain IV interact with
353 the anticodon stem-loop of the A-site tRNA during translocation (*24, 35*) and mutations in this domain slow
354 the rate of translocation (*19, 46*). It is therefore an enticing hypothesis that EF-G may have an additional
355 role in mRNA frame maintenance in addition to its established function in translocation.

356 Although all three prokaryotic $tRNA^{Pro}$ isoacceptors have the capacity to frameshift, whether they
357 use similar mechanisms of action is unknown (*8, 11, 13*). The m^1G37 modification minimally influences
358 frameshifting in proline isoacceptor $tRNA^{Pro}_{GGG}$ (*proL*) in contrast to $tRNA^{Pro}_{cmo^5UGG}$ (*proM*) (*11*). An additional
359 difference is the dependency on elongation factor-P (EF-P) to reconcile +1 frameshifts. EF-P binds at the
360 E site to overcome ribosome stalling induced by poly-proline codons (*47, 48*) and is critical in suppressing
361 frameshifts on poly-proline stretches (*11*). While EF-P reduces +1 frameshifts with $tRNA^{Pro}_{GGG}$ G37 (Δm^1) to
362 an equivalent frequency as native $tRNA^{Pro}_{GGG}$, there is little influence on isoacceptor $tRNA^{Pro}_{cmo^5UGG}$ in the absence
363 or presence of m^1G37 (*11*). These mechanistic differences may be due to a combination of the codon-
364 anticodon pairings on slippery codons ($tRNA^{Pro}_{cmo^5UGG}$ and $tRNA^{Pro}_{GGG}$ are cognate with slippery codons while
365 $tRNA^{Pro}_{CGG}$ is near-cognate (*49*)) and/or the influence of other modifications such as the cmo^5-U34
366 modification in $tRNA^{Pro}_{cmo^5UGG}$ (*50*). Our structures show that regardless of the m^1G37 modification status of

367 $tRNA^{Pro}_{CGG}$, the near-cognate slippery codon causes the tRNA to be destabilized, biasing its position towards
368 the E site, which we predict is indicative of high levels of frameshifting. The possible synergistic effects of
369 cmo^5-U34 and m^1G37 in $tRNA^{Pro}_{cmo^5UGG}$ in preventing frameshifts is unclear, but $tRNA^{Pro}_{UGG}$ lacking all
370 modifications exhibits higher levels of frameshifting than $tRNA^{Pro}_{UGG}$ lacking only the m^1G37 modification
371 (*43*). Also, m^1G37 in $tRNA^{Pro}_{cmo^5UGG}$ may prevent movement to the e*/E position where it may not be an optimal
372 substrate for EF-P, which would be consistent with kinetic analyses (*11*). Since unmodified $tRNA^{Pro}_{UGG}$ would
373 be near-cognate on a slippery sequence without the cmo^5-U34, it is reasonable to hypothesize that the major
374 species of unmodified $tRNA^{Pro}_{CGG}$ would also frameshift, during translocation to the P site or in the P site, in
375 agreement with the structural work presented here.
376

377 **MATERIALS AND METHODS**

378 **mRNA, ASL and ribosome purification.** ASL^{Pro} containing a m^1G37 modified anticodon stem-loop (18
379 nucleotides) and mRNA (19 nucleotides) were purchased from GE Healthcare Dharmacon and dissolved
380 in 10 mM Tris-HCl, pH 7.0 and 5 mM $MgCl_2$. We used a chemically synthesized 17-nucleotide ASL to
381 ensure complete m^1G modification at position 37, as previously used to examine interactions in the A site
382 (*14*). Purification of *Thermus thermophilus* 70S ribosomes was performed as previously described (*51*).
383

384 **$tRNA^{Pro}_{CGG}$ ligation and purification.** To ensure that $tRNA^{Pro}_{CGG}$ was methylated at tRNA nucleotide 37 (m^1G),
385 the 5' half of the tRNA (nucleotides 1-39) was chemically synthesized (GE Healthcare Dharmacon) and
386 enzymatically ligated to the chemically synthesized 3' half following established protocols (*52, 53*). Briefly,
387 T4 polynucleotide kinase (NEB) was used to phosphorylate the 5' end of the 3' tRNA half and was heat
388 inactivated. The 5' and 3' halves of each tRNA were then mixed and annealed in the T4 RNA ligase buffer
389 by heating to 80 ºC for 5 mins and slow cooling on the heat block to room temperature. T4 RNA ligase
390 (NEB) was added to the reaction at 37 ºC for 18 hours. The ligation reaction was run on a 12% denaturing
391 8M urea-polyacrylamide gel and the ligated fragment was excised and purified using a modified crush and
392 soak method (*53*). The RNA was ethanol precipitated, the pellet was thoroughly air dried and resuspended

393 in 10 mM Tris-HCl, pH 7.0 and 5 mM $MgCl_2$, followed by annealing at 70 ºC for 2 min and slow cooled
394 to room temperature on the benchtop. The purified full-length RNA was aliquoted and stored at -20 ºC.
395
396 **Structural studies.** ASL^{Pro} complexes were formed with 3.5 µM 70S ribosomes programmed with 7 µM
397 mRNA for 6 min at 37 ºC. Then 22 µM ASL^{Pro} was added and incubated for 30 min at 55 ºC. $tRNA^{Pro}_{CGG}$ and
398 $tRNA^{Pro}_{CGG}$ Δm^1G complexes were formed with 3.5-4.4 µM of 70S ribosomes programmed with 7-10.5 µM
399 mRNA for 6 min at 37 ºC. Then 7.7-10.5 µM $tRNA^{Pro}_{CGG}$ or $tRNA^{Pro}_{CGG}$ Δm^1G were incubated for 30 min at 55
400 ºC. Each ASL and tRNA were programmed in the ribosomal P site by designing the Shine-Dalgarno
401 sequence five nucleotides upstream of the P-site codon. Crystals were grown by sitting-drop vapor diffusion
402 in a 1:1 drop ratio of 100 mM Tris–acetate pH 7.6, 12–13% 2-methyl-2,4-pentanediol (MPD), 2.9-3.0%
403 polyethylene glycol (PEG) 20K, 100-150 mM L-arginine-HCl and 0.5-1 mM β-mercaptoethanol (β-Me).
404 ASL^{Pro} crystals were cryoprotected step-wise in 100 mM Tris–acetate pH 7.6, 10 mM NH_4Cl, 50 mM KCl,
405 3.1% PEG 20K, 10 mM $Mg(CH_3COO)_2$, 6 mM β-Me and 20%-40% MPD, with the final cryoprotection
406 solution containing 30 µM ASL^{Pro}. Cryoprotection of $tRNA^{Pro}_{CGG}$ and $tRNA^{Pro}_{CGG}$ Δm^1G was accomplished
407 similarly to ASL^{Pro}, except with 3% PEG 20K and 20 mM $Mg(CH_3COO)_2$. Additionally, the final
408 cryoprotection solution for both $tRNA^{Pro}_{CGG}$ and $tRNA^{Pro}_{CGG}$ Δm^1G did not contain ligand. All crystals were flash
409 frozen in liquid nitrogen for data collection.
410 X-ray diffraction data were collected at the Southeast Regional Collaborative Access Team (SER-
411 CAT) 22-ID beamline line and the Northeastern Collaborative Access Team (NE-CAT) ID24-C and ID24-
412 E beamlines at the Advanced Photon Source (APS). Data were integrated and scaled using the program
413 XDS (*54*). All structures of 70S-ASL^{Pro} and $tRNA^{Pro}_{CGG}$ containing cognate mRNA were solved by molecular
414 replacement in PHENIX using coordinates from a 70S structure containing mRNA and tRNAs (Table S1)
415 (PDB code 4V6G) (*55, 56*). For the 70S complex containing an e*/E tRNA and the mRNA, the start model
416 was changed to $tRNA^{SufA6}$ bound to slippery sequence (PDB code 5VPP) (*18*). In this structure, the 30S
417 head domain is swiveled ~18º relative to the 50S. The structure was solved by molecular replacement in

418 PHENIX followed by iterative rounds of manual building in Coot (*57*). All figures were prepared in PyMOL
419 (*58*).

420 **Calculating 30S head movement.** The following protocol was used to describe the 30S head and body
421 domains in terms of Euler angles (ϕ,ψ,θ). Here, $\phi+\psi$ defines the net swivel angle, tilting is described by θ
422 and the tilt direction is defined by ϕ. Euler angles were calculated separately for the 16S body and head
423 domains as previously defined (*34*). Briefly, for all calculations, the P atoms of the "core" residues of the
424 23S rRNA and 16S head/body were considered. The core residues are defined as the set of atoms that were
425 found to have spatial root mean squared fluctuations of less than 1 Å in a 1 microsecond explicit-solvent
426 simulation (*59*). This includes 1351, 442 and 178 residues in the 23S rRNA, 16S body and 16S head,
427 respectively. To ensure that the calculated angles reflect global domain orientations, rather than local
428 deformations, reference configurations of the 23S, as well as the 16S head and body, were aligned to each
429 group of core residues, separately. To calculate 16S body swivel angles, each model was first aligned to a
430 crystallographic model of a classical unrotated ribosome (PDB codes 4V9D:DA and 4V9D:BA), where
431 alignment was based on the 23S rRNA core atoms. To define the orientation of the body, axes were
432 constructed based on the aligned orientations of residues 41, 127 and 911, which are used to define the
433 plane of rotation. The Euler angles are then calculated based on the orientational difference of the fitted
434 axes in the reference classical configuration and the structural model of interest. To describe the orientation
435 of the head, the 16S body was first aligned to the reference model (alignment based on core atoms) and
436 axes were defined based on residue 984, 940 and 1106. According to these definitions, models (4V9D:DA,
437 4V9D:BA) and (4V9D:CA, 4V9D:AA) define pure (tilt-free) body rotation, and models (4V9D:DA,
438 4V9D:BA) and (4V4Q:DB, 4V4Q:CA) define pure (tilt-free) head swivel. The classical model (4V9D:DA,
439 4V9D:BA) is defined as the zero-tilt, zero-rotation orientation.
440

441 **ACKNOWLEDGMENTS**

442 We thank Ha An Nguyen, Jacob Mattingly, Pooja Srinivas, Dr. Alexandra Kuzmishin Nagy and Dr. Graeme
443 L. Conn for critical reading of the manuscript, and the staff members of the NE-CAT and SER-CAT
444 beamlines for assistance during data collection. This work was supported by the NIH (R01GM093278 (to
445 CMD), NIH R01GM119386 (to RLG), and NSF MCB-1915843 (PW). CMD is a Burroughs Wellcome
446 Fund Pathogenesis of Infectious Diseases Fellow. The x-ray crystallography datasets were collected at the
447 NE-CAT beamlines, which are funded by the National Institute of General Medical Sciences from the NIH
448 (P41 GM103403), and at the SER-CAT beamlines. The Pilatus 6M detector on 24-IDC beamline is funded
449 by a NIH-ORIP HEI grant (S10 RR029205). This research used resources of the Advanced Photon Source,
450 a US Department of Energy (DOE) Office of Science User Facility operated for the DOE Office of Science
451 by Argonne National Laboratory under contract no. DE-AC02-06CH11357.

FIGURE LEGENDS

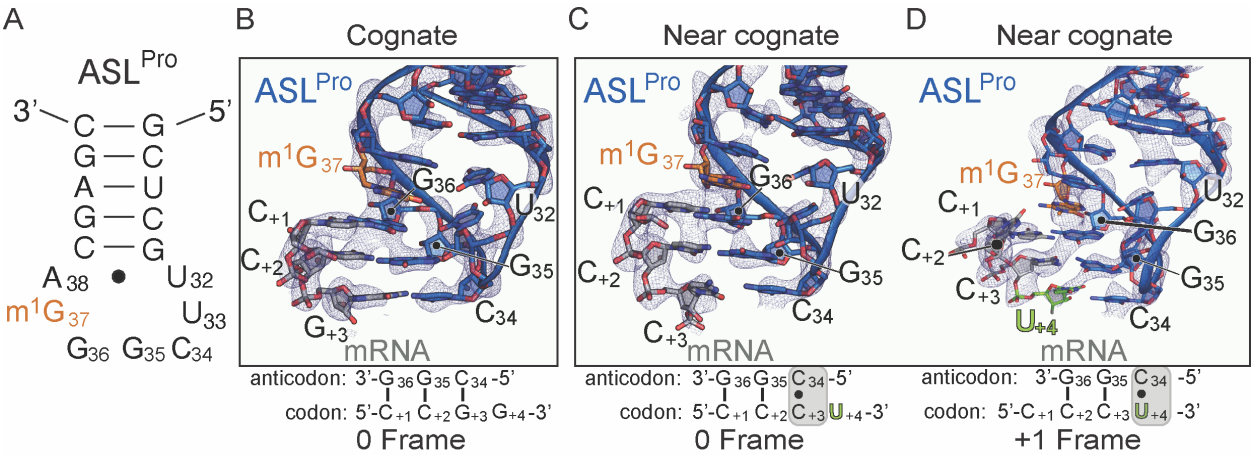

Figure 1. The ability of ASL^{Pro} to +1 frameshift in the peptidyl (P) site is dependent on the near-cognate mRNA codon. (A) Secondary structure of the anticodon stem-loop (ASL) of tRNA^{Pro}. The m^{1}G37 modified nucleotide is shown in orange and the anticodon nucleotides (C34, G35, and G36) and the U32-A38 pairing are labeled. (B) Structure of 70S-ASL^{Pro} bound to a cognate CCG codon in the P site with the codon in the 0 or canonical frame. All $2F_o$-F_c electron density maps shown in panels B-D are contoured at 1.0 sigma. (C,D) Structure of 70S-ASL^{Pro} bound to a +1 slippery, near-cognate CCC-U codon shows the mRNA position is either in the 0 (panel C) or +1 frame (panel D) in the two 70S molecules in the crystallographic asymmetric unit. In either the 0 or +1 frame, a *cis* Watson-Crick interaction at the third base-pair forms (C_{+3}•C34 or U_{+4}•C34). mRNA numbering starts at +1 according to the first position in the P site.

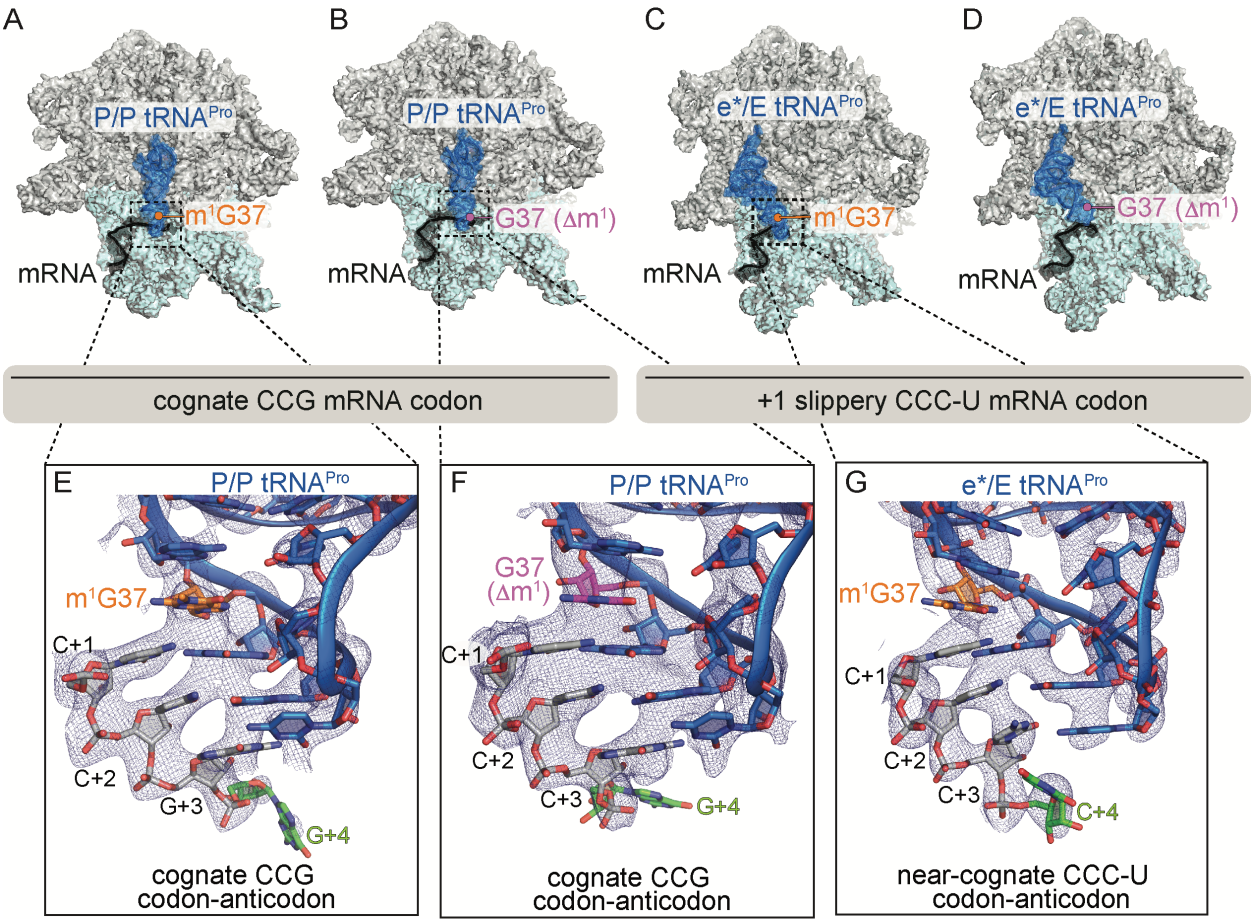

Figure 2. Identity of the mRNA proline codon regulates 30S head domain movement. Overview of 70S ribosome-tRNA^{Pro} complex structures: (A) tRNA^{Pro} m^{1}G37 on a cognate CCG codon adopts a P/P orientation (in the P site on the 30S and 50S subunits); (B) tRNA^{Pro} lacking the m^{1}G37 modification (G37 Δm^1) on a cognate CCG codon also adopts a P/P orientation; (C) tRNA^{Pro} on a slippery, near-cognate CCC-U codon adopts an e*/E orientation; and (D) tRNA^{Pro} lacking the m^{1}G37 (G37 Δm^1) on a slippery, near-cognate CCC-U codon adopts an e*/E orientation. In this complex (panel D), the 30S head domain and anticodon-codon interaction are disordered. In panels A-D, the 16S rRNA of the 30S head domain is removed for clarity. Zoomed in view of $2F_o$-F_c density of (E) the codon-anticodon for tRNA^{Pro} on a cognate CCG codon, (F) tRNA^{Pro} G37 Δm^1 on a cognate CCG codon in the P site, and (G) tRNA^{Pro} G37 Δm^1 on a near-cognate CCC-U codon in position between the E and the P sites (e*). All $2F_o$-F_c electron density maps shown in panels E-G are contoured at 1.0 sigma.

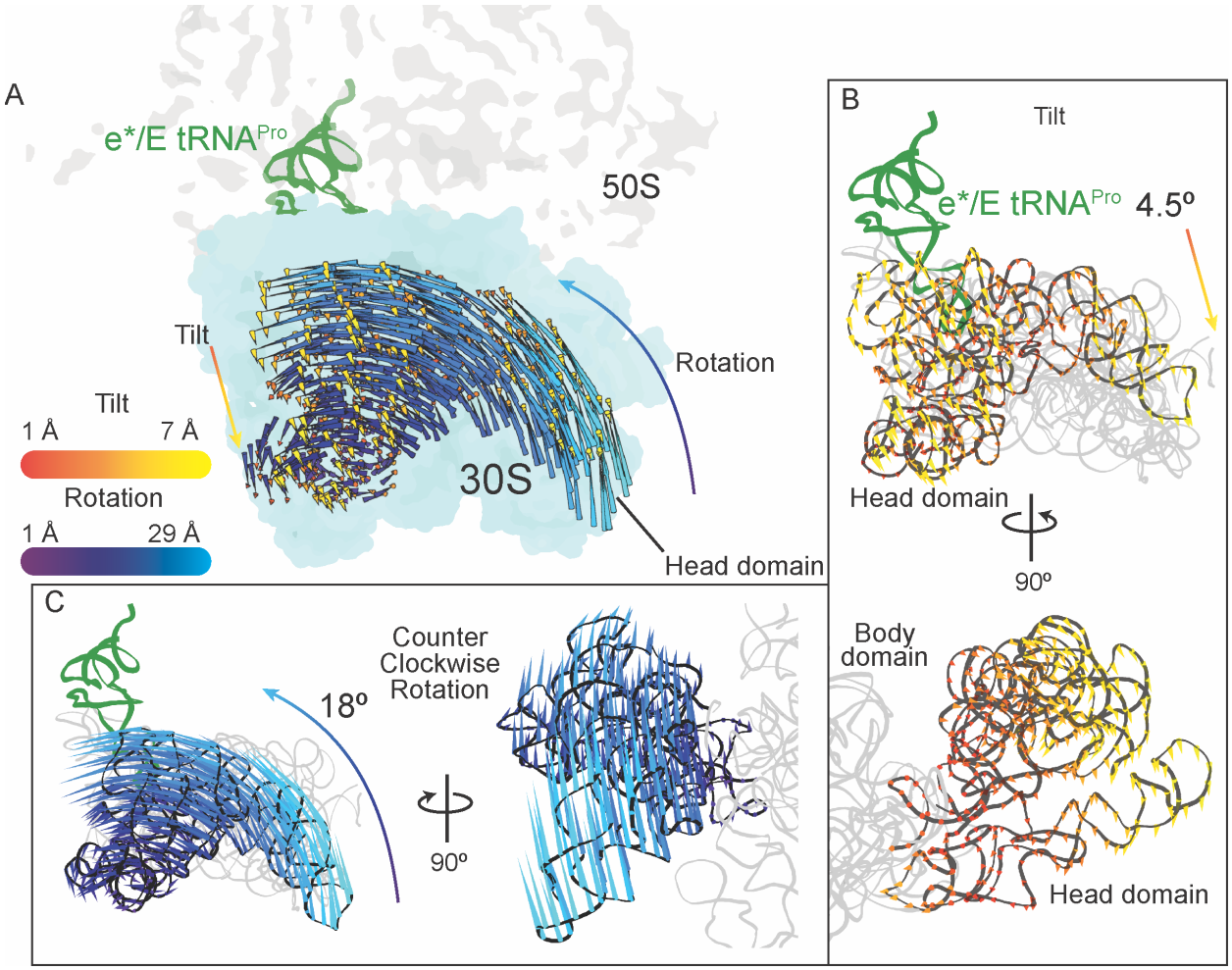

Figure 3. 30S head domain movement in the presence of a +1 frameshift-prone tRNA. (A) Overview of the 70S ribosome containing an e*/E tRNA^{Pro} bound to a slippery, near-cognate CCC-U codon. Shifts in phosphate atom positions of the 30S head domain (16S rRNA nucleotides 930-1380) in this structure as compared to the unrotated 70S (PDB code 4V5C). (B) *Top*, same view as in panel A but showing only the tilt of the head domain . *Bottom*, a 90° rotated view showing tilting is downward resulting in movement of the head domain away from the body domain. (C) *Left*, the same view as in panel A with only the counterclockwise swivel of the head domain indicated (left). *Right*, a 90° horizontal rotated view indicates the swivel is greatest towards the subunit interface, close to e*/E tRNA^{Pro} and on the surface.

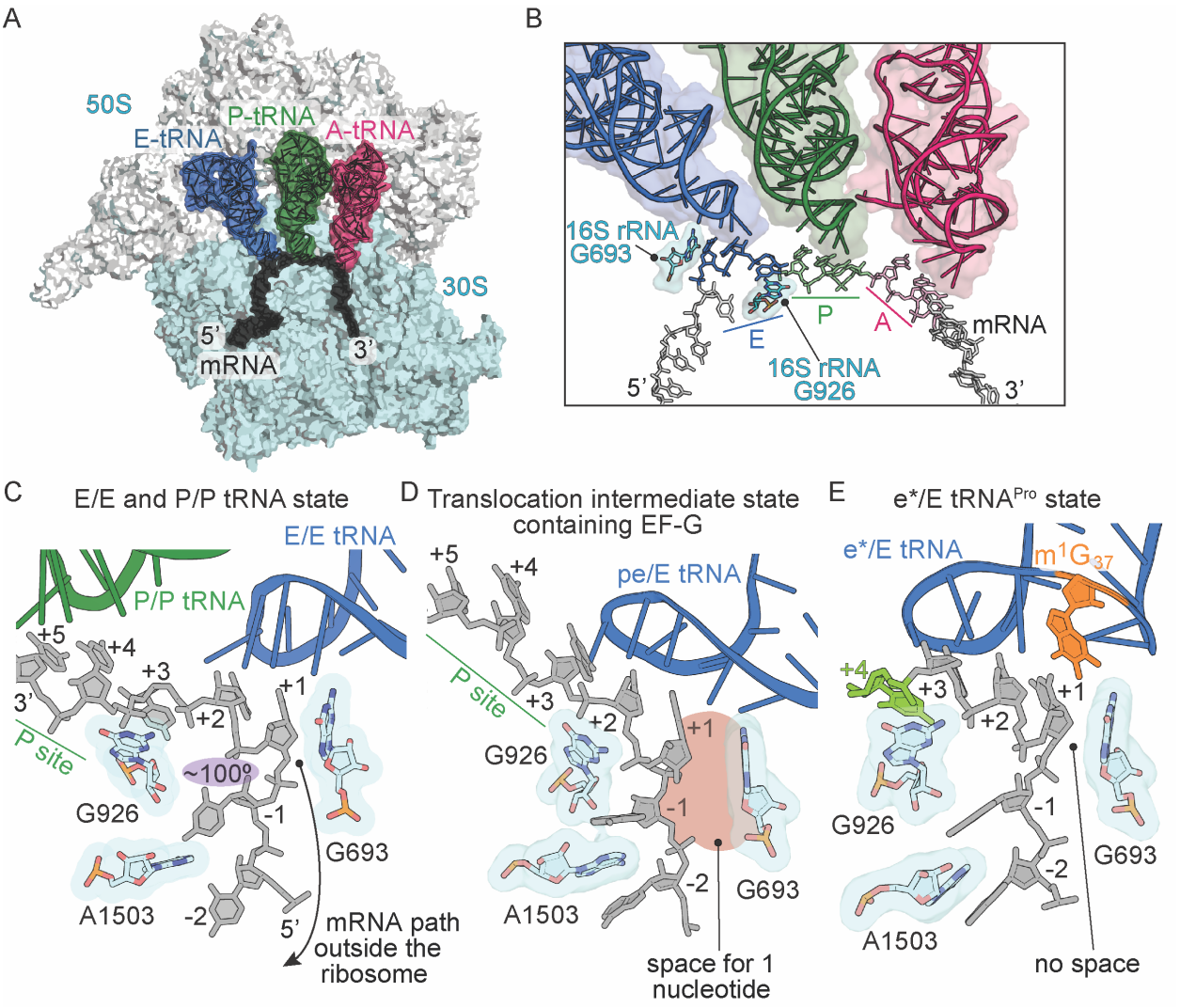

Figure 4. Frame-dependent conformations of the mRNA in the E and P sites. (A) Overview of the 70S ribosome with (B) a zoomed in view of the tRNA-mRNA interaction in the A, P and E sites (PDB code 4V6F). 16S rRNA nucleotides G693 and G926 interact with the E-site codon-anticodon. (C) The normal path of the mRNA (grey) in a ribosome structure containing P/P and E/E tRNAs demonstrates only a three-nucleotide codon (nucleotides +1, +2 and +3) is accommodated in the E site (PDB code 4V5F). 16S rRNA G693 defines the starts of the E-site codon and interacts with the first nucleotide. As the mRNA leaves the E site, there is a 100° kink between the first nucleotide of the E-site codon (+1) and the -1 nucleotide (shaded in purple). Panel C is rotated ~180° relative to the view in panel B. (D) A translocation intermediate state induced by EF-G contains a tRNA positioned between the P and the E sites on the 30S (denoted "pe"). The

pe/E tRNA has not undergone full translocation to the E site and thus only two nucleotides (+1 and +2) are located in the E site (PDB code 4W29). In this translocation intermediate state, there is space available to accommodate an additional nucleotide of the codon (shaded in red). (E) $tRNA^{Pro}$ bound to a +1 slippery CCC-U codon reveals that although the codon-anticodon pair has not been fully translocated, this placement of the mRNA is different as compared to normal translocation intermediates structures as shown in panel D. The additional nucleotide (+4) of the four-nucleotide codon is shown in green.

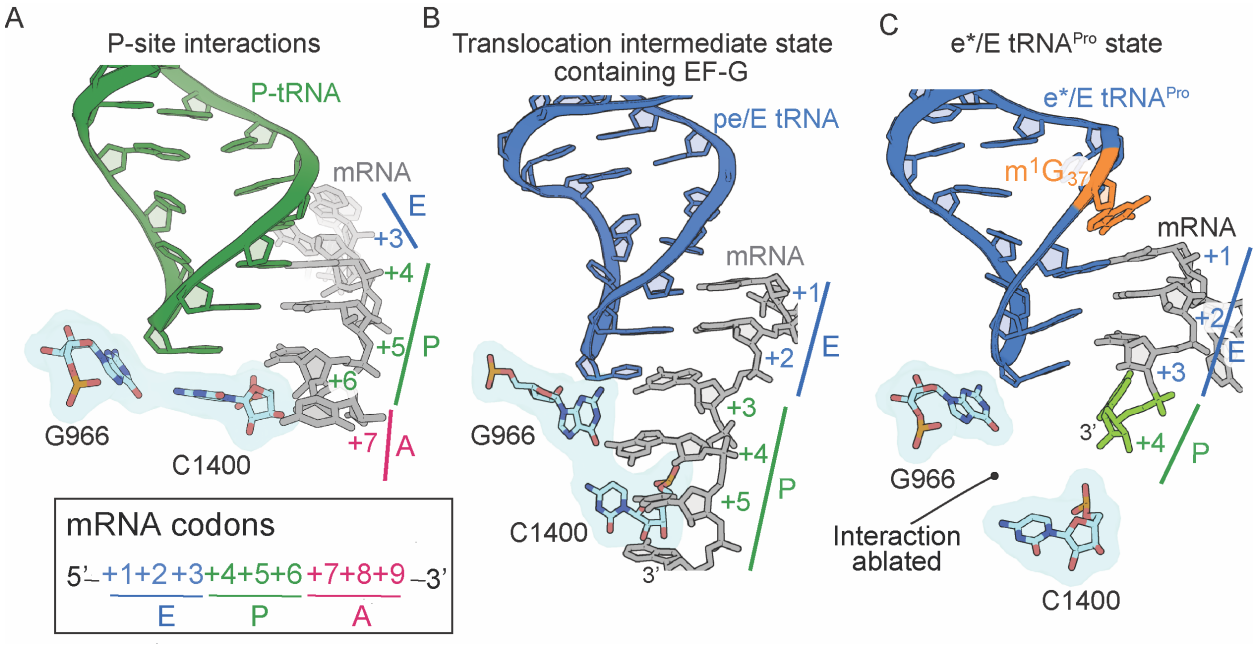

Figure 5. The 16S rRNA G966-C1400 gate between the 30S head and body domains is disrupted during a frameshift event. (A) In a post-translocation state containing E/E, P/P and A/A tRNAs, 16S rRNA nucleotides G966 and C1400 interaction forms beneath the P-site tRNA (PDB code 4V5F). (B) The G966 and C1400 interaction persists during EF-G-mediated translocation as the position of 30S head domain nucleotide G966 shifts while 30S body nucleotide C1400 remains constant (PDB code 4W29). (C) In a ribosome undergoing a +1 frameshift induced by $tRNA^{Pro}$ and a slippery CCC-U codon, the G966-C1400 interaction is broken. The additional nucleotide (+4) of the four nucleotide codon is shown in green.

TABLES

Table 1: RNAs used in this study.

$tRNA^{Pro}$ 5' half	5'-CGGUGAUUGGCGCAGCCUGGUAGCGCACUUCGUUCGGm[1]GA-3'
$tRNA^{Pro}$ 3' half	5'-CGAAGGGGUCGGAGGUUCGAAUCCUCUAUCACCGACCA-3'
mRNA_cognate	5'- GGCA<u>AGGAG</u>GUAAAA **CCG**G-3'
mRNA_slippery	5'- GGCA<u>AGGAG</u>GUAAAA **CCCU**-3'

The underlined nucleotides indicates the Shine-Dalgarno region while the bold nucleotides are the P-site codons.

Table 2. Data collection and refinement statistics for 70S-ASL^{Pro} structures.

	70S-ASL^{Pro}-CCG codon	**70S-ASL^{Pro} CCC-U codon**
Data collection		
Space group	$P2_12_12_1$	$P2_12_12_1$
Wavelength (Å)	0.9791	0.9791
Cell dimensions		
a, b, c (Å)	209.79 451.91 621.58	210.12451.80 622.96
α, β, γ (°)	90, 90, 90	90, 90, 90
Resolution (Å)	49.70 - 3.10 (3.21 - 3.10)	49.70 - 3.40 (3.52 - 3.40)
R_{pim} (%)	21.2(80.5)	14.5(65.5)
I/σI	4.7(1.1)	5.9(1.3)
Completeness (%)	97.99 (87.41)	98.85 (94.87)
Redundancy	3.7(3.1)	4.2(3.4)
CC1/2	0.968(0.250)	0.987(0.359)
Refinement		
Reflections	1034968 (91757)	797600 (75973)
R_{work}/R_{free} (%)	24.1/27.2	19.8/23.7
No. atoms	289313	290047
B-factors (Å^2)		
Overall	90.37	103.79
Macromolecule	90.6	104.05
Ligand/ion	39.43	43.84
R.m.s deviations		
Bond lengths (Å)	0.004	0.010
Bond angles (°)	0.83	0.98
PDB ID	6NTA	6NSH

Highest resolution shell is shown in parentheses.

Table 3. Data collection and refinement statistics for 70S-tRNA^{Pro} structures

	tRNA^{Pro} m^{1}G37 CCG codon	tRNA^{Pro} m^{1}G37 CCC-U codon	tRNA^{Pro} G37 (Δm^1) CCG codon	tRNA^{Pro} G37 (Δm^1) CCC-U codon
Data collection				
Space group	$P2_12_12_1$	$P2_12_12_1$	$P2_12_12_1$	$P2_12_12_1$
Wavelength (Å)	0.9792	0.9792	0.9792	0.9792
Cell dimensions				
a, b, c (Å)	210.20 451.47 620.21	210.74 450.26 626.11	209.97 450.71 619.40	210.09 450.32 622.89
α, β, γ (°)	90, 90, 90	90, 90, 90	90, 90, 90	90, 90, 90
Resolution (Å)	49.20 - 3.20 (3.31 - 3.20)	49.93 - 3.50 (3.63 - 3.50)	49.82 - 3.97 (4.11 - 3.97)	49.83 - 4.14 (4.288 - 4.14)
R_{pim} (%)	11.5(51.7)	9.00(44.1)	8.60(86.0)	9.807 (95.5)
I/σI	6.7(1.5)	7.8(1.7)	6.3(1.0)	5.1 (1.0)
Completeness (%)	99.11 (98.45)	97.55 (89.72)	98.60 (95.72)	98.39 (95.63)
Redundancy	5.9(4.4)	4.2(2.2)	14.1(10.0)	6.5 (3.6)
CC1/2	0.991(0.377)	0.996(0.464)	0.998(0.313)	0.998 (0.37)
Refinement				
Reflections	951115 (93932)	723555 (66052)	4959167(47742)	439195 (42360)
R_{work}/R_{free} (%)	22.8/25.6	23.4/25.6	22.8/25.5	24.8/29.4
No. atoms	291966	292039	291793	291185
B-factors (Å^2)				
Overall	103.87	113.6	177.39	247.09
Macromolecule	104.12	113.9	177.77	247.54
Ligand/ion	42.04	37.71	72.42	123.12
R.m.s deviations				
Bond lengths (Å)	0.011	0.010	0.007	0.007
Bond angles (°)	1.00	1.23	0.94	1.38
PDB ID	6NUO	6NWY	6O3M	6OSI

Highest resolution shell is shown in parentheses.

VIDEO LEGENDS

Video 1. mRNA frameshifting of ASL^{Pro} to +1 mRNA reading frame in the peptidyl (P) site is dependent on the slippery mRNA codon. An overview of the 70S ribosome (50S is light cyan and the 30S in grey) showing how the anticodon stem-loop (ASL) of tRNA^{Pro} (blue) interacts with either a cognate CCG codon or a slippery CCC-U codon (black). The m^{1}G37 modified nucleotide is shown in orange. A zoomed-in view of the anticodon nucleotides (G36, G35, and C34) interacting with the cognate C_{+1}, C_{+2} and G_{+3} mRNA respectively, in the 0 frame. All $2F_o$-F_c electron density maps shown are contoured at 1.0 sigma. A morph from the 0 frame structure to the structure of ASL^{Pro} interacting with a slippery CCC-U codon is shown to demonstrate the movement in the mRNA into the +1 frame. The fourth nucleotide of the mRNA codon is shown in green. In either the 0 or +1 frame, a *cis* Watson-Crick interaction at the third base-pair forms (C_{+3}•C34 or U_{+4}•C34). mRNA numbering starts at +1 according to the first position in the P site.

Video 2. Influence of m^{1}G37 and the slippery codon on +1 frameshifting and conformational changes 30S head domain. An overview of the 70S ribosome (50S is light cyan and the 30S in grey) showing how tRNA^{Pro} (blue) (+/- m^{1}G37) interacts with either a cognate CCG codon or a slippery CCC-U codon (black). A zoomed-in view of the anticodon nucleotides (G36, G35, and C34) interacting with the cognate C_{+1}, C_{+2} and G_{+3} mRNA respectively, in the 0 frame. All $2F_o$-F_c electron density maps shown are contoured at 1.0 sigma. The m^{1}G37 modified nucleotide is shown in orange and the U32-A38 pairing is indicated. A morph of the changes of the U32-A38 pairing when the tRNA interacts with either a cognate CCG or a slippery CCC-U codon is shown. An overview and a morph of P/P tRNA^{Pro} bound to a cognate CCG codon to the e*/E site is shown along with movement of the 30S head domain is shown. Lastly, a zoomed in view shows a morph from a 0 frame interaction that forms in the P/P site to the codon-anticodon interaction as the pairing is in the e*/E site.

REFERENCES

1. P. F. Agris, A. Narendran, K. Sarachan, V. Y. P. Vare, E. Eruysal, The Importance of Being Modified: The Role of RNA Modifications in Translational Fidelity. *Enzymes* **41**, 1-50 (2017).
2. P. Boccaletto, M. A. Machnicka, E. Purta, P. Piatkowski, B. Baginski, T. K. Wirecki, V. de Crecy-Lagard, R. Ross, P. A. Limbach, A. Kotter, M. Helm, J. M. Bujnicki, MODOMICS: a database of RNA modification pathways. 2017 update. *Nucleic Acids Res* **46**, D303-D307 (2018).
3. P. F. Agris, E. R. Eruysal, A. Narendran, V. Y. P. Vare, S. Vangaveti, S. V. Ranganathan, Celebrating wobble decoding: Half a century and still much is new. *RNA biology* **15**, 537-553 (2018).
4. M. A. Machnicka, A. Olchowik, H. Grosjean, J. M. Bujnicki, Distribution and frequencies of post-transcriptional modifications in tRNAs. *RNA biology* **11**, 1619-1629 (2014).
5. F. V. t. Murphy, V. Ramakrishnan, A. Malkiewicz, P. F. Agris, The role of modifications in codon discrimination by tRNA(Lys)UUU. *Nat Struct Mol Biol* **11**, 1186-1191 (2004).
6. M. Sundaram, P. C. Durant, D. R. Davis, Hypermodified nucleosides in the anticodon of tRNA(Lys) stabilize a canonical U-turn structure. *Biochemistry* **39**, 15652 (2000).
7. H. A. Nguyen, E. D. Hoffer, C. M. Dunham, Importance of a tRNA anticodon loop modification and a conserved, noncanonical anticodon stem pairing in tRNACGGProfor decoding. *J Biol Chem* **294**, 5281-5291 (2019).
8. G. R. Bjork, P. M. Wikstrom, A. S. Bystrom, Prevention of translational frameshifting by the modified nucleoside 1-methylguanosine. *Science* **244**, 986-989 (1989).
9. J. Li, B. Esberg, J. F. Curran, G. R. Bjork, Three modified nucleosides present in the anticodon stem and loop influence the in vivo aa-tRNA selection in a tRNA-dependent manner. *Journal of molecular biology* **271**, 209-221 (1997).
10. J. Urbonavicius, Q. Qian, J. M. Durand, T. G. Hagervall, G. R. Bjork, Improvement of reading frame maintenance is a common function for several tRNA modifications. *Embo J* **20**, 4863-4873 (2001).
11. H. B. Gamper, I. Masuda, M. Frenkel-Morgenstern, Y. M. Hou, Maintenance of protein synthesis reading frame by EF-P and m(1)G37-tRNA. *Nature communications* **6**, 7226 (2015).
12. G. E. Sroga, F. Nemoto, Y. Kuchino, G. R. Bjork, Insertion (sufB) in the anticodon loop or base substitution (sufC) in the anticodon stem of tRNA(Pro)2 from Salmonella typhimurium induces suppression of frameshift mutations. *Nucleic Acids Res* **20**, 3463-3469 (1992).
13. Q. Qian, J. N. Li, H. Zhao, T. G. Hagervall, P. J. Farabaugh, G. R. Bjork, A new model for phenotypic suppression of frameshift mutations by mutant tRNAs. *Mol Cell* **1**, 471-482 (1998).
14. T. Maehigashi, J. A. Dunkle, S. J. Miles, C. M. Dunham, Structural insights into +1 frameshifting promoted by expanded or modification-deficient anticodon stem loops. *Proc Natl Acad Sci U S A* **111**, 12740-12745 (2014).
15. S. S. Phelps, C. Gaudin, S. Yoshizawa, C. Benitez, D. Fourmy, S. Joseph, Translocation of a tRNA with an extended anticodon through the ribosome. *Journal of molecular biology* **360**, 610-622 (2006).
16. S. E. Walker, K. Fredrick, Recognition and positioning of mRNA in the ribosome by tRNAs with expanded anticodons. *Journal of molecular biology* **360**, 599-609 (2006).
17. C. E. Fagan, T. Maehigashi, J. A. Dunkle, S. J. Miles, C. M. Dunham, Structural insights into translational recoding by frameshift suppressor tRNASufJ. *RNA* **20**, 1944-1954 (2014).
18. S. Hong, S. Sunita, T. Maehigashi, E. D. Hoffer, J. A. Dunkle, C. M. Dunham, Mechanism of tRNA-mediated +1 ribosomal frameshifting. *Proc Natl Acad Sci U S A* **115**, 11226-11231 (2018).
19. M. V. Rodnina, A. Savelsbergh, V. I. Katunin, W. Wintermeyer, Hydrolysis of GTP by elongation factor G drives tRNA movement on the ribosome. *Nature* **385**, 37-41 (1997).
20. D. N. Ermolenko, H. F. Noller, mRNA translocation occurs during the second step of ribosomal intersubunit rotation. *Nat Struct Mol Biol* **18**, 457-462 (2011).

21. M. R. Wasserman, J. L. Alejo, R. B. Altman, S. C. Blanchard, Multiperspective smFRET reveals rate-determining late intermediates of ribosomal translocation. *Nat Struct Mol Biol* **23**, 333-341 (2016).
22. R. Belardinelli, H. Sharma, N. Caliskan, C. E. Cunha, F. Peske, W. Wintermeyer, M. V. Rodnina, Choreography of molecular movements during ribosome progression along mRNA. *Nat Struct Mol Biol* **23**, 342-348 (2016).
23. A. H. Ratje, J. Loerke, A. Mikolajka, M. Brunner, P. W. Hildebrand, A. L. Starosta, A. Donhofer, S. R. Connell, P. Fucini, T. Mielke, P. C. Whitford, J. N. Onuchic, Y. Yu, K. Y. Sanbonmatsu, R. K. Hartmann, P. A. Penczek, D. N. Wilson, C. M. Spahn, Head swivel on the ribosome facilitates translocation by means of intra-subunit tRNA hybrid sites. *Nature* **468**, 713-716 (2010).
24. J. Zhou, L. Lancaster, J. P. Donohue, H. F. Noller, Crystal structures of EF-G-ribosome complexes trapped in intermediate states of translocation. *Science* **340**, 1236086 (2013).
25. J. Zhou, L. Lancaster, J. P. Donohue, H. F. Noller, How the ribosome hands the A-site tRNA to the P site during EF-G-catalyzed translocation. *Science* **345**, 1188-1191 (2014).
26. W. Holtkamp, C. E. Cunha, F. Peske, A. L. Konevega, W. Wintermeyer, M. V. Rodnina, GTP hydrolysis by EF-G synchronizes tRNA movement on small and large ribosomal subunits. *EMBO J* **33**, 1073-1085 (2014).
27. R. Belardinelli, H. Sharma, F. Peske, W. Wintermeyer, M. V. Rodnina, Translocation as continuous movement through the ribosome. *RNA biology* **13**, 1197-1203 (2016).
28. M. Selmer, C. M. Dunham, F. V. t. Murphy, A. Weixlbaumer, S. Petry, A. C. Kelley, J. R. Weir, V. Ramakrishnan, Structure of the 70S ribosome complexed with mRNA and tRNA. *Science* **313**, 1935-1942 (2006).
29. H. S. Zaher, R. Green, Quality control by the ribosome following peptide bond formation. *Nature* **457**, 161-166 (2009).
30. H. Grosjean, D. G. Soll, D. M. Crothers, Studies of the complex between transfer RNAs with complementary anticodons. I. Origins of enhanced affinity between complementary triplets. *Journal of molecular biology* **103**, 499-519 (1976).
31. E. M. Gustilo, F. A. Vendeix, P. F. Agris, tRNA's modifications bring order to gene expression. *Curr Opin Microbiol* **11**, 134-140 (2008).
32. S. Mohan, J. P. Donohue, H. F. Noller, Molecular mechanics of 30S subunit head rotation. *Proc Natl Acad Sci U S A* **111**, 13325-13330 (2014).
33. J. Zhou, L. Lancaster, J. P. Donohue, H. F. Noller, Spontaneous ribosomal translocation of mRNA and tRNAs into a chimeric hybrid state. *Proc Natl Acad Sci U S A* **116**, 7813-7818 (2019).
34. K. Nguyen, P. C. Whitford, Steric interactions lead to collective tilting motion in the ribosome during mRNA-tRNA translocation. *Nature communications* **7**, 10586 (2016).
35. Y. G. Gao, M. Selmer, C. M. Dunham, A. Weixlbaumer, A. C. Kelley, V. Ramakrishnan, The structure of the ribosome with elongation factor G trapped in the posttranslocational state. *Science* **326**, 694-699 (2009).
36. C. Yarian, H. Townsend, W. Czestkowski, E. Sochacka, A. J. Malkiewicz, R. Guenther, A. Miskiewicz, P. F. Agris, Accurate translation of the genetic code depends on tRNA modified nucleosides. *J Biol Chem* **277**, 16391-16395 (2002).
37. T. G. Hagervall, T. M. Tuohy, J. F. Atkins, G. R. Bjork, Deficiency of 1-methylguanosine in tRNA from Salmonella typhimurium induces frameshifting by quadruplet translocation. *Journal of molecular biology* **232**, 756-765 (1993).
38. J. D. Dinman, Control of gene expression by translational recoding. *Advances in protein chemistry and structural biology* **86**, 129-149 (2012).
39. J. A. Dunkle, C. M. Dunham, Mechanisms of mRNA frame maintenance and its subversion during translation of the genetic code. *Biochimie* **114**, 90-96 (2015).

40. J. F. Atkins, G. Loughran, P. R. Bhatt, A. E. Firth, P. V. Baranov, Ribosomal frameshifting and transcriptional slippage: From genetic steganography and cryptography to adventitious use. *Nucleic Acids Res*, (2016).
41. N. Korniy, E. Samatova, M. M. Anokhina, F. Peske, M. V. Rodnina, Mechanisms and biomedical implications of -1 programmed ribosome frameshifting on viral and bacterial mRNAs. *FEBS letters* **593**, 1468-1482 (2019).
42. J. M. Ogle, F. V. Murphy, M. J. Tarry, V. Ramakrishnan, Selection of tRNA by the ribosome requires a transition from an open to a closed form. *Cell* **111**, 721-732 (2002).
43. H. B. Gamper, I. Masuda, M. Frenkel-Morgenstern, Y. M. Hou, The UGG Isoacceptor of tRNAPro Is Naturally Prone to Frameshifts. *Int J Mol Sci* **16**, 14866-14883 (2015).
44. J. A. Dunkle, L. Wang, M. B. Feldman, A. Pulk, V. B. Chen, G. J. Kapral, J. Noeske, J. S. Richardson, S. C. Blanchard, J. H. Cate, Structures of the bacterial ribosome in classical and hybrid states of tRNA binding. *Science* **332**, 981-984 (2011).
45. N. M. Abdi, K. Fredrick, Contribution of 16S rRNA nucleotides forming the 30S subunit A and P sites to translation in Escherichia coli. *Rna* **11**, 1624-1632 (2005).
46. A. Savelsbergh, N. B. Matassova, M. V. Rodnina, W. Wintermeyer, Role of domains 4 and 5 in elongation factor G functions on the ribosome. *Journal of molecular biology* **300**, 951-961 (2000).
47. S. Ude, J. Lassak, A. L. Starosta, T. Kraxenberger, D. N. Wilson, K. Jung, Translation elongation factor EF-P alleviates ribosome stalling at polyproline stretches. *Science* **339**, 82-85 (2013).
48. P. Huter, S. Arenz, L. V. Bock, M. Graf, J. O. Frister, A. Heuer, L. Peil, A. L. Starosta, I. Wohlgemuth, F. Peske, J. Novacek, O. Berninghausen, H. Grubmuller, T. Tenson, R. Beckmann, M. V. Rodnina, A. C. Vaiana, D. N. Wilson, Structural Basis for Polyproline-Mediated Ribosome Stalling and Rescue by the Translation Elongation Factor EF-P. *Mol Cell* **68**, 515-527 e516 (2017).
49. S. J. Nasvall, P. Chen, G. R. Bjork, The modified wobble nucleoside uridine-5-oxyacetic acid in tRNAPro(cmo5UGG) promotes reading of all four proline codons in vivo. *RNA* **10**, 1662-1673 (2004).
50. I. Masuda, R. Takase, R. Matsubara, M. J. Paulines, H. Gamper, P. A. Limbach, Y. M. Hou, Selective terminal methylation of a tRNA wobble base. *Nucleic Acids Res* **46**, e37 (2018).
51. Y. Zhang, S. Hong, A. Ruangprasert, G. Skiniotis, C. M. Dunham, Alternative Mode of E-Site tRNA Binding in the Presence of a Downstream mRNA Stem Loop at the Entrance Channel. *Structure* **26**, 437-445 e433 (2018).
52. L. D. Sherlin, T. L. Bullock, T. A. Nissan, J. J. Perona, F. J. Lariviere, O. C. Uhlenbeck, S. A. Scaringe, Chemical and enzymatic synthesis of tRNAs for high-throughput crystallization. *RNA* **7**, 1671-1678 (2001).
53. M. R. Stark, S. D. Rader, Efficient splinted ligation of synthetic RNA using RNA ligase. *Methods Mol Biol* **1126**, 137-149 (2014).
54. W. Kabsch, Xds. *Acta crystallographica* **66**, 125-132 (2010).
55. L. B. Jenner, N. Demeshkina, G. Yusupova, M. Yusupov, Structural aspects of messenger RNA reading frame maintenance by the ribosome. *Nat Struct Mol Biol* **17**, 555-560 (2010).
56. P. D. Adams, P. V. Afonine, G. Bunkoczi, V. B. Chen, I. W. Davis, N. Echols, J. J. Headd, L. W. Hung, G. J. Kapral, R. W. Grosse-Kunstleve, A. J. McCoy, N. W. Moriarty, R. Oeffner, R. J. Read, D. C. Richardson, J. S. Richardson, T. C. Terwilliger, P. H. Zwart, PHENIX: a comprehensive Python-based system for macromolecular structure solution. *Acta crystallographica* **66**, 213-221 (2010).
57. P. Emsley, B. Lohkamp, W. G. Scott, K. Cowtan, Features and development of Coot. *Acta crystallographica* **66**, 486-501 (2010).
58. Schrodinger, LLC. (2010).
59. P. C. Whitford, S. C. Blanchard, J. H. Cate, K. Y. Sanbonmatsu, Connecting the kinetics and energy landscape of tRNA translocation on the ribosome. *PLoS Comput Biol* **9**, e1003003 (2013).